

(REVIEW ARTICLE)



Grid-connected photovoltaic system dispatch using full bridge inverter with two control loops

Hassnen. S. H. Senoussi ^{1,*}, Abdulgader Alsharif ², Abdussalam Ali Ahmed ², Ibrahim Imbayah ³ and Maamar Miftah Rahmah ⁴

¹ Department of Electrical and Electronic Engineering, Faculty of Technical Sciences Sabha, Sabha, Libya.

² Department of Mechanical Engineering, Bani Waleed University, Bani Waleed, Libya.

³ Department of Energy Engineering, College of Renewable Energy, Tajoura, Libya.

⁴ Mellitah Oil and Gas Company, Tripoli, Libya.

World Journal of Advanced Engineering Technology and Sciences, 2023, 10(02), 096–111

Publication history: Received on 12 October 2023; revised on 26 October 2023; accepted on 29 November 2023

Article DOI: <https://doi.org/10.30574/wjaets.2023.10.2.0295>

Abstract

In rural areas that are remote from power transmission lines, Photovoltaic (PV) systems are almost a must for any power system in order to supply electricity through independent systems. The surrounding environment, including temperature and sun radiation, has an impact on photovoltaic systems that generate electricity. For this reason, these systems employ Maximum Power Point Tracking (MPPT) techniques. This document offers a comprehensive analysis of the relationship between the grid and PV systems, beginning with the relationship between the circuit and PV cell, which includes the converter for Buck With the help of a three-phase converter that synchronizes the PV system with the utility power grid using two control loops (voltage-current), DC-DC operates with the Perturb and Observation (P&O) algorithm for MPPT applied to a 120kW PV array. All of the earlier parts were linked to the utility power grid via a three-phase converter, which synchronizes the PV system with the grid and feeds it with active power with a power factor of one using two voltage-current control loops. MATLAB/Simulink was used to apply the simulation outcome.

Keywords: Photovoltaic; Three phase transformer; MPPT; P&O; Buck converter

1. Introduction

Concerning the environmental effects of traditional power plants, the penetration of Renewable Energy Systems (RES) has grown in the last two decades, PV systems and wind turbines are the most common types of renewable energy generating systems. The PV systems consist of standalone and grid-connected systems [1]. Moreover, grid-connected systems contain large-scale (centralized) or small-scale (distributed) systems [2]. The absorbed power from PV systems is highly changed with the amount of temperature and irradiance for solar [3], we have many Maximum Power Point Tracking (MPPT) techniques being used with it, such as Neural networks [4], Fuzzy logic, Perturb and Observation (P&O) algorithm, incremental conductance, Constant voltage and open circuit voltage etc..[5]. The converter of DC-DC is an important component in PV systems, it adjusts the output voltage of a Photovoltaic panel on a fixed value or for varying values as in the case of MPP tracking, there are many kinds of DC-DC converters are being used to have higher or lower voltage from the PV such as Buck-Boost, Boost, Cuk, Buck, and SEPIC etc..[6], [7]. For connecting two or more electrical power systems there are four essential conditions that must be fulfilled, In PV systems the centralized inverter is responsible for this operation [8].

In the first section of this paper, the aim of the article is positioned along with five parameters circuit of a PV cell were introduced, and then we will model a 120kW PV array, the second part P&O algorithm has been used for control of the

* Corresponding author: Hassnen. S. H. Senoussi

cycle at the converter, the converter of third party for DC-DC Buck works with the algorithm of the P&O, the fourth is a three-phase inverter with two control loops were modelled to apply the role of interface between the grid and Photovoltaic. The remaining sections of the paper are organized as follows. The PV cell description is positioned in Section 2. Section 3 presents the Perturb and Observation (P&O) algorithm along with the flowchart and mathematical equations of the aforementioned method. The Buck converter details are placed in Section 4. The main operation structure of the proposed system appears in Section 5. The obtained results and its discussion are located in Section 6 along with the sub sections. Section 7 discussing the case study. Finally, the summary conclusion of the article is presented followed by cited references.

2. PV Cell

For this paper we will use a single diode with series resistance and parallel resistance for modelling the operation of a PV cell. This model will use both series resistance (R_s) and the second resistance for the PV system, the handle one is R_{sh} [9]. The realistic results had been obtained. The equivalent circuit of PV Cell is represented in Figure 1.

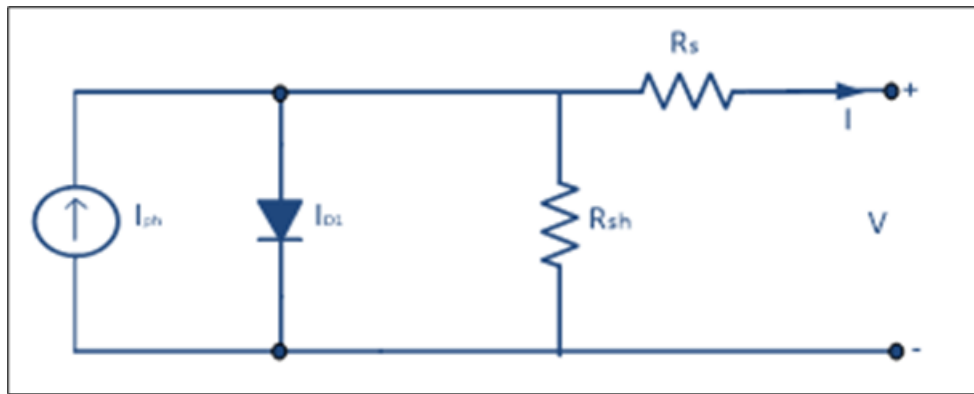


Figure 1 Circuit of PV cell includes R_{sh} and R_s

The value of output current for PV is described with the expression:

$$I = I_{ph} - I_d - I_{sh} \dots\dots\dots(1)$$

Taking into account the expressions for the I_d and I_{sh} , we will solve. The intensity of current produced by photovoltaic system into the load has this characteristic:

$$I_d = I_0 \left(\exp \frac{q(V+IR_s)}{n K T_{op}} - 1 \right) \dots\dots\dots(2)$$

$$I_{sh} = \frac{(V+R_s I)}{R_{sh}} \dots\dots\dots(3)$$

$$I = I_{ph} - I_0 \left(\exp \frac{q(V+IR_s)}{n K T_{op}} - 1 \right) - \frac{(V+R_s I)}{R_{sh}} \dots\dots\dots(4)$$

K refer to Boltzmann constant, n denotes as the factor of the Diode $1 < n < 2$, q is the Electron Charge 1.6021×10^{-19} , I_{ph} represents the photocurrent, I_0 stand for saturation of Diode current, T indicates the operation temperature.

3. The Algorithm OF P&O MPPT

The P&O is an repeated method for the track of MPP [10], [11]. The operation is depending on periodic measures for current and the voltage of PV system to knows the system power; the value will compared with previous power values, the voltage of operating for the system is modified [12]. When the array of power will increase ($dP/dV > 0$), we can control and adjusts the PV system for array of operating point in this direction, or the operating point will move to the opposite direction. This process is continuously repeated until the MPP is reached; the system keeps oscillating around this point. Figure 2 shows the flowchart of P&O algorithm [13].

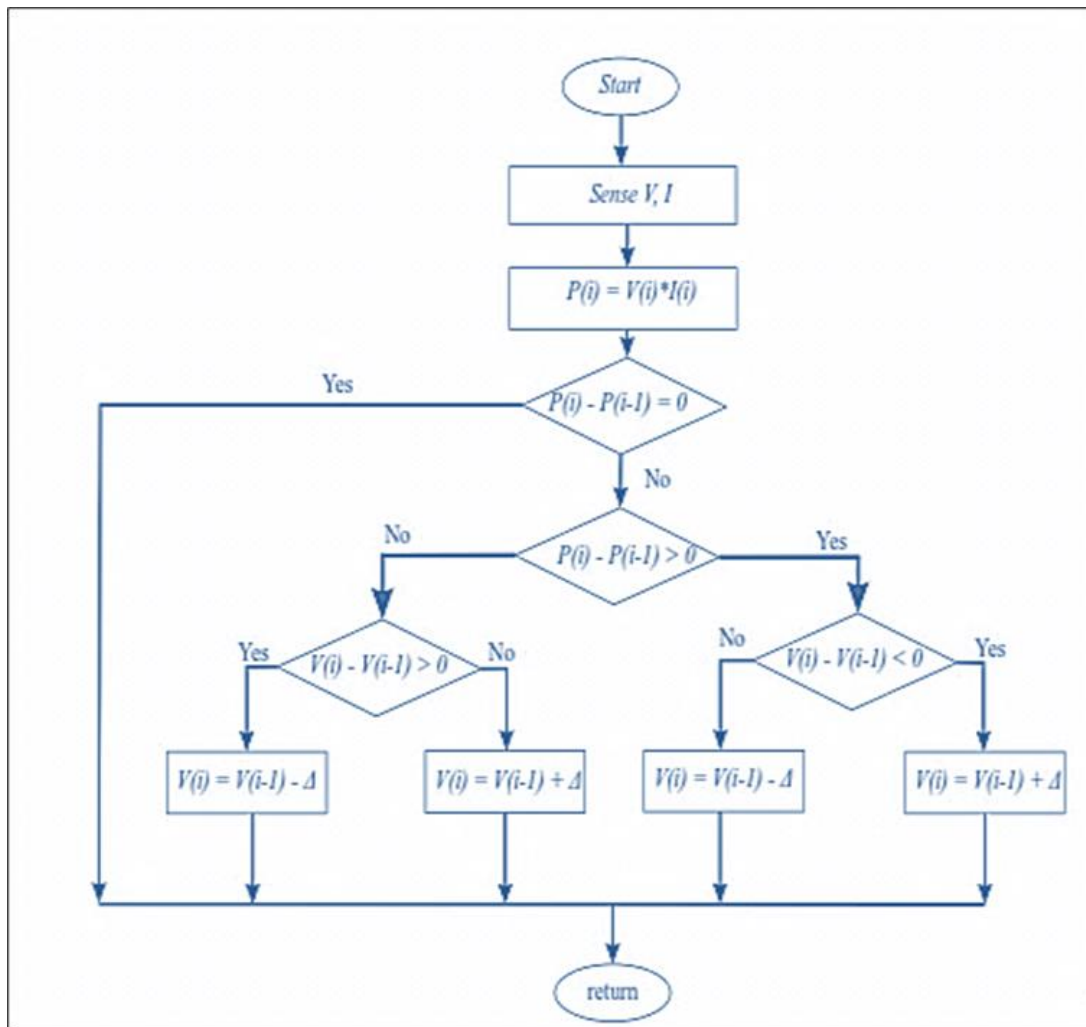


Figure 2 Flowchart of P&O MPPT method

4. BUCK Converter

The converter for DC-DC buck operates in a step-down direction, it means will step down the high voltage for input to the low voltage for output, the magnitude of the output voltage is always lower than the input voltage. This converter will connect to low voltage DC of load or for the bank of battery from a high PV array voltage.

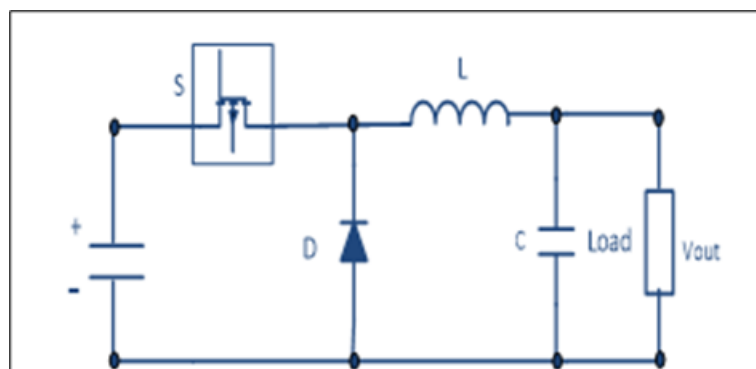


Figure 3 Circuit topology of DC-DC buck converter

The converters of DC-DC buck are used in so high range step down and low power range regulators of converters, because it's simple of topology with low control, and less number for components with no isolation. Most of the DC-DC

buck converters are used for charging of the battery when the high input voltage is modulated through PWM to generate the required of low output voltage for the batteries, while the MPP tracking is ordered to maximize of the output power which obtained from the PV arrays. Figure 3 the basic of circuit topology for DC-DC Buck converter [14].

The output voltage is expressed in Eq. (5) and D indicates the duty cycle.

$$V_{out} = D \cdot V_{in} \dots \dots \dots (5)$$

5. Proposed Control Structure

The controller consists of two control loops, the first one is the voltage regulator which controls the amplitude of voltage supply in the output using transformations of two axes (d, q), and the second loop is current control which regulates the active power provided by the system at unity power factor or less depending on dispatch parameters. The use of two independent Loops in the controller helps in the process of regulating the voltage supply and injecting the active or reactive power separately. Figure 4 shows the general layout of the used controller which depends on the equations of the modelling inverter. The concept of the Utility Grid effort and the basic value of Voltage and Active power for using PU, the voltage and current values from the photovoltaic system were calculated using the PU system before conversion to the two rotating axis (d,q) [15]. The phase lock technique PLL was used to obtain angle velocity (wt). Since the work of the controller is dependent on the rotary (dq) theory, it is necessary to make park’s transformations for network voltage and the current generated by the PV system. The regulator of voltage adjusts the alternating current voltage and determines reference value (i_{d-ref}), Where the active power provided by the system relates to the value of the current i_d and voltage v_d .

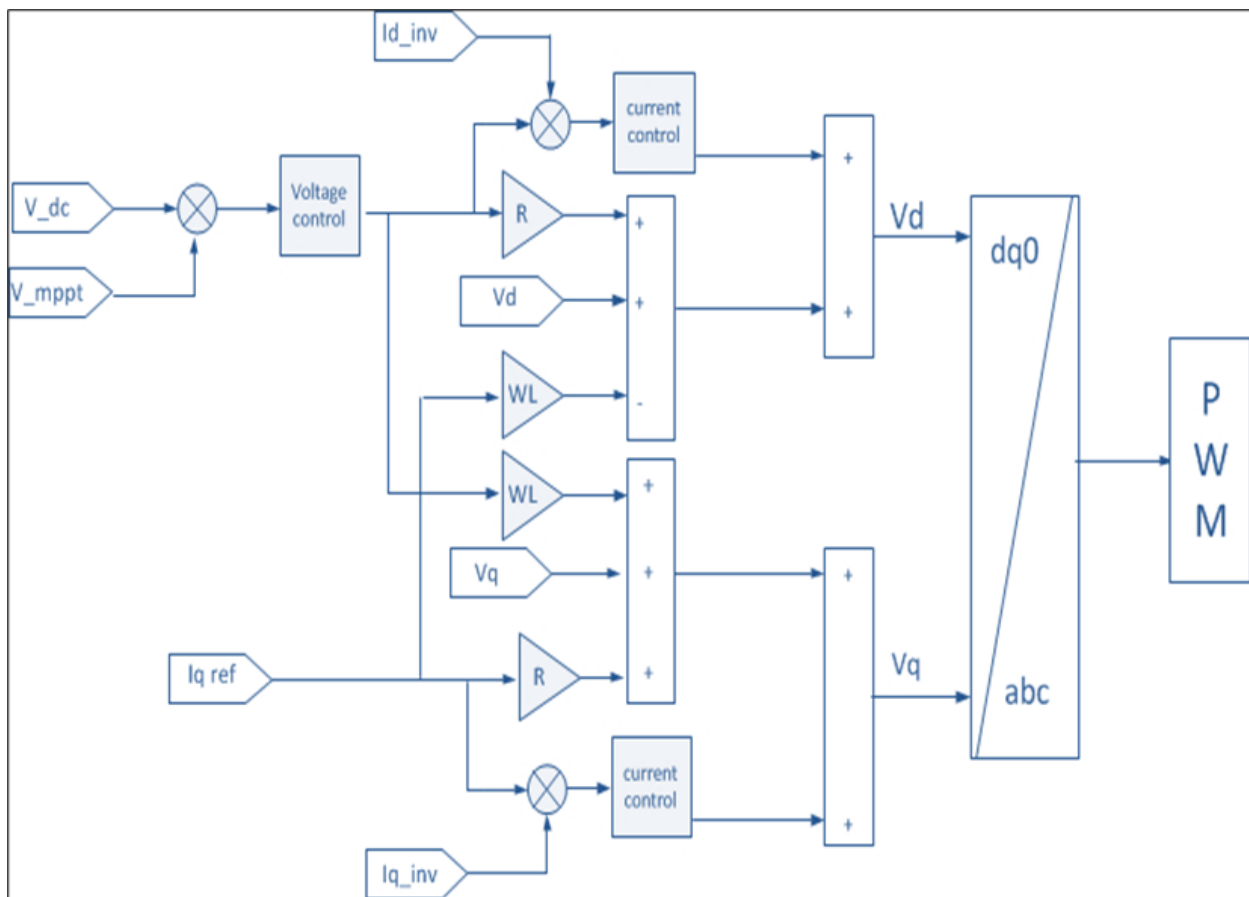


Figure 4 Proposed Control structure

The voltage regulator ensures that the active power is provided to the utility grid, by adjusting the voltage amplitude and not passing the power in the opposite direction. For the current controller, it determines the value of currents $i_d i_q$ to be provided from the PV system [16]. The active and reactive power capacity is given with the d,q axis:

$$P = V_d i_d + V_q i_q \quad \& \quad Q = V_q i_d - V_d i_q \dots \dots \dots (6)$$

The reference value $i_{q-ref} = 0$ is then taken to provide active power for the unity of power factor. When finding the value of $V_q V_d$ in the rotating sentence, we convert it to the sentence (a, b, c) to determine the reference sinusoidal signal used to generate PWM pulses. The outline of the control of the key is given in Figure 5.

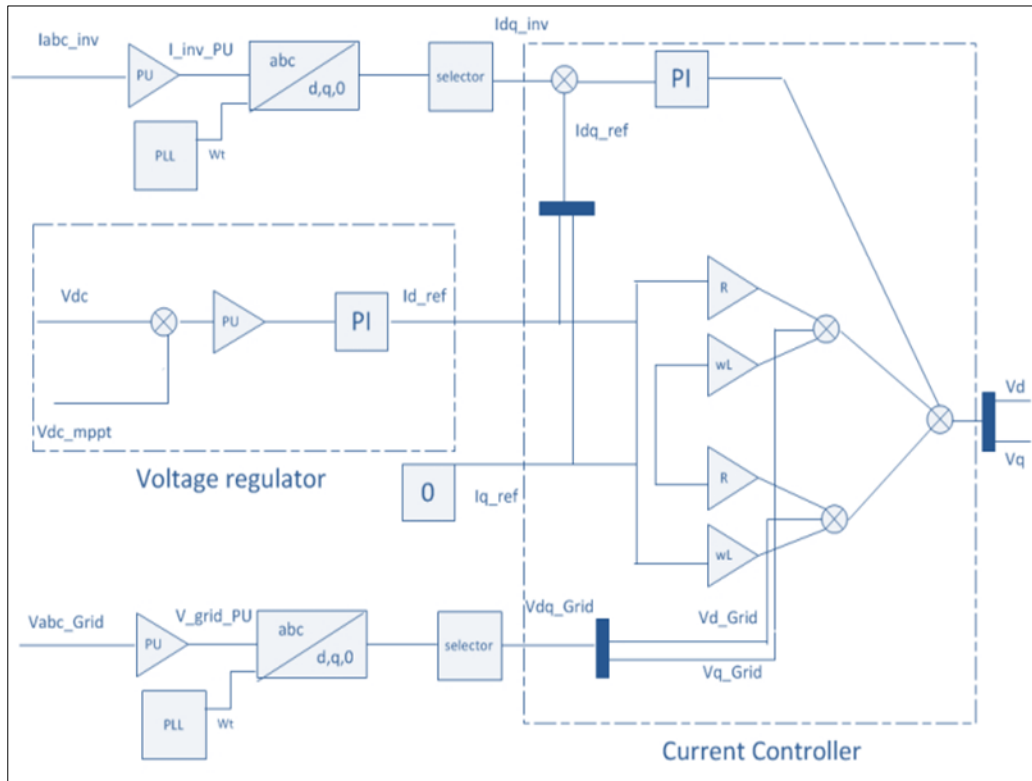


Figure 5 Detailed structure of the controller

6. Simulation and Results

6.1. Five Parameters Model

Using Five parameters equivalent Circuit and equations for studying the performance of PV panel as presented in Table 1 under different of values for the Solar irradiance and the temperature, we use the same constants of the PV panel for (Samsung SDIPV-MBA1CG255) from MATLAB/Simulink 2017 which are:

Table 1 Five parameters model

I_{sc}	V_{oc}	V_{mpp}	P_{max}	n
8.89A	38.1 V	30.5 V	255w	60 cell

Figure 6 shows the simulation of PV cell equations:

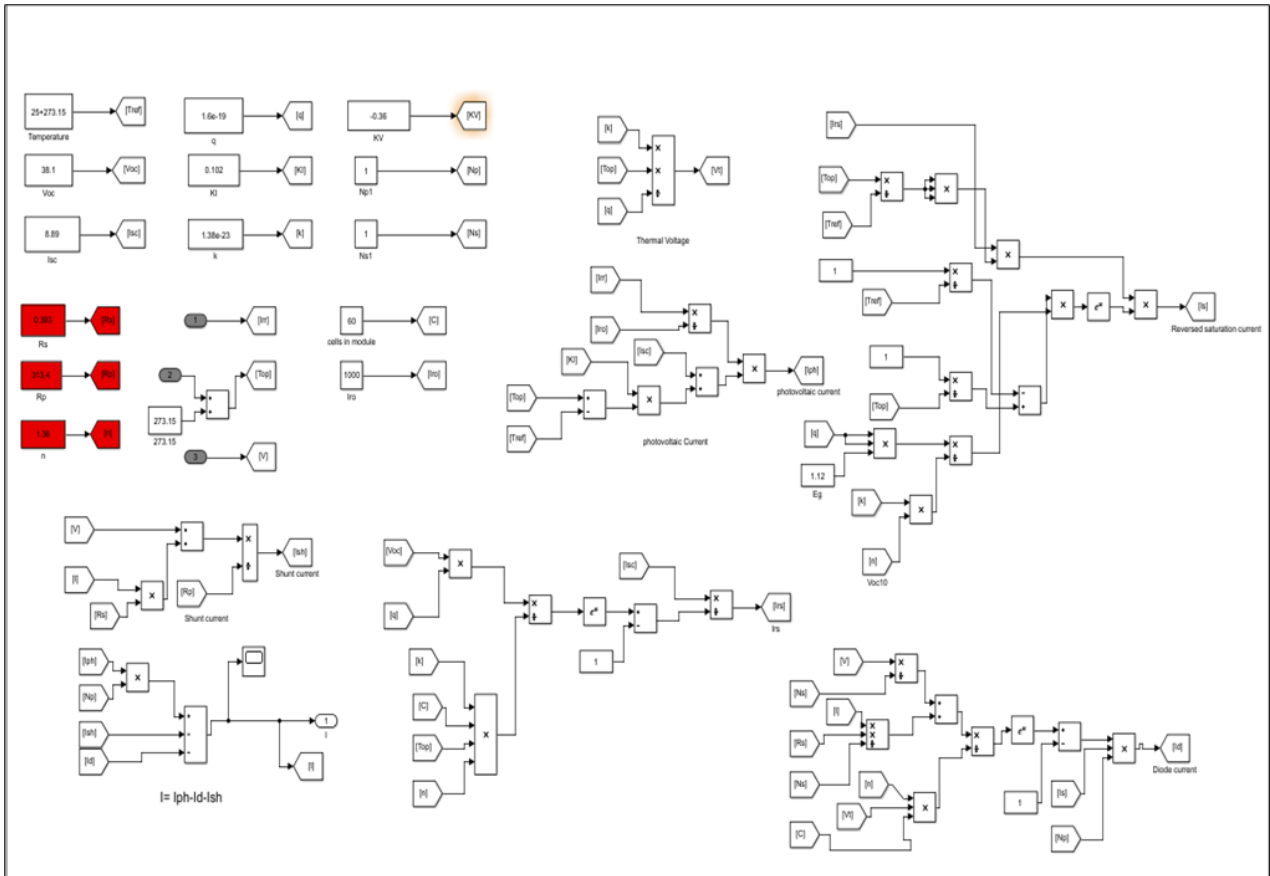


Figure 6 Simulation of PV cell

We will put all these equations in subsystem and connect it to current source, we will have the electrical output of PV cell as shown in Figure 7.

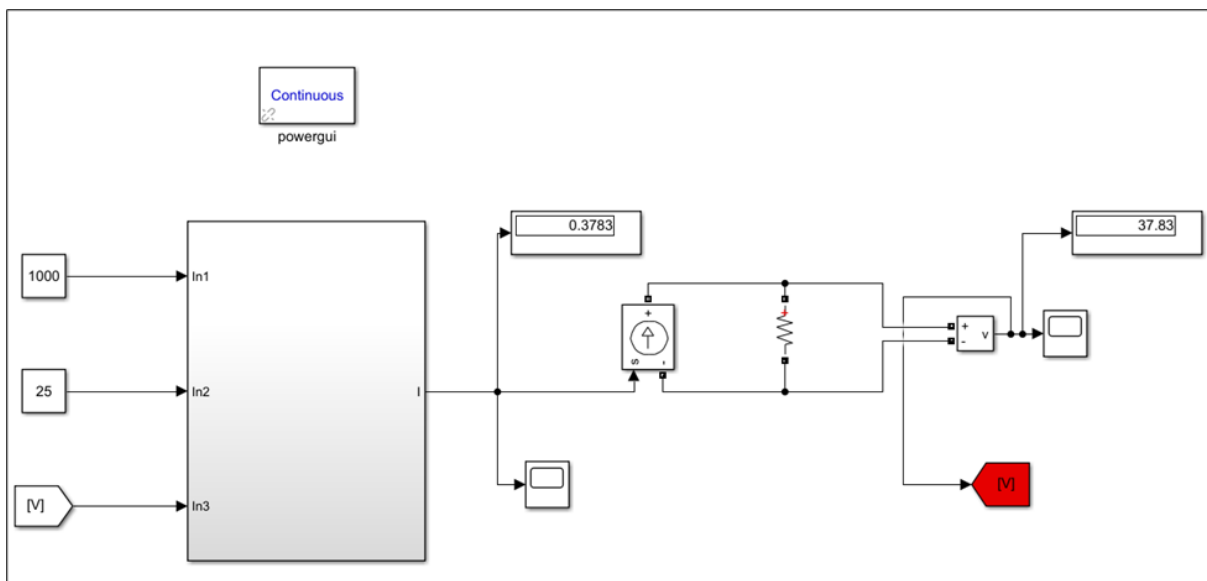


Figure 7 PV module simulation

Under different Values of solar irradiance [1000-600-400] the output voltage is in Figure 8.

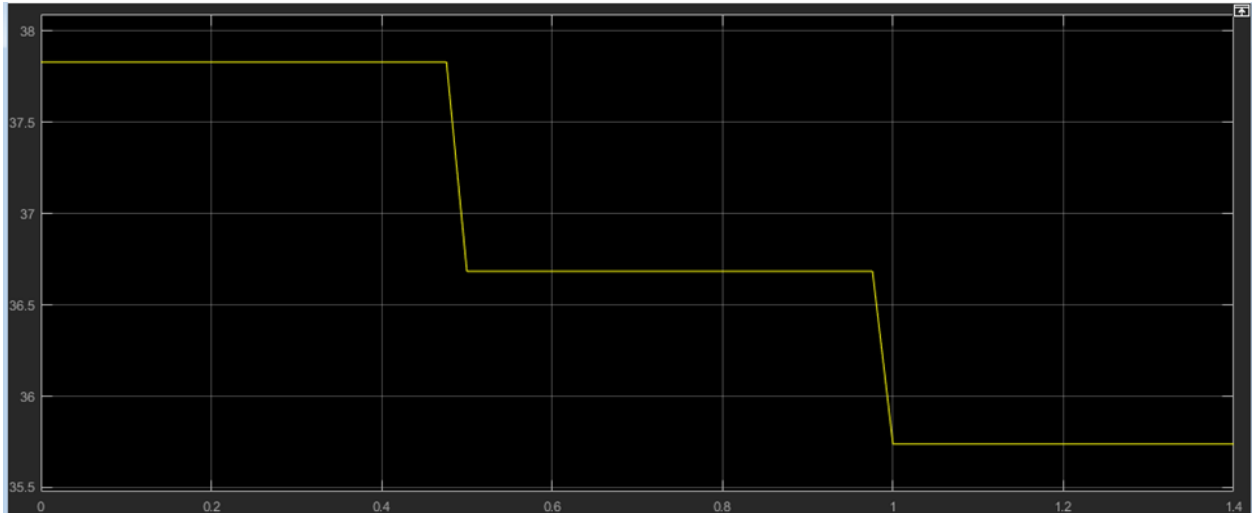


Figure 8 Output voltage

6.2. P&O- MPPT Algorithm with buck converter

Applying P&O algorithm as a function in MATLAB/Simulink to control the Buck converter, the input variables are I_{pv} , V_{pv} , T (time of sampling), the function will compare the output power according to the changes of Duty Cycle and will decide to increase or decrease it. As the result we will use the maximum load (Resistance), it's worth to mention the P&O applied directly on the Gate of the transistor on the Buck converter [17]. The simulation for PV system with MPPT are being in Figure 9.

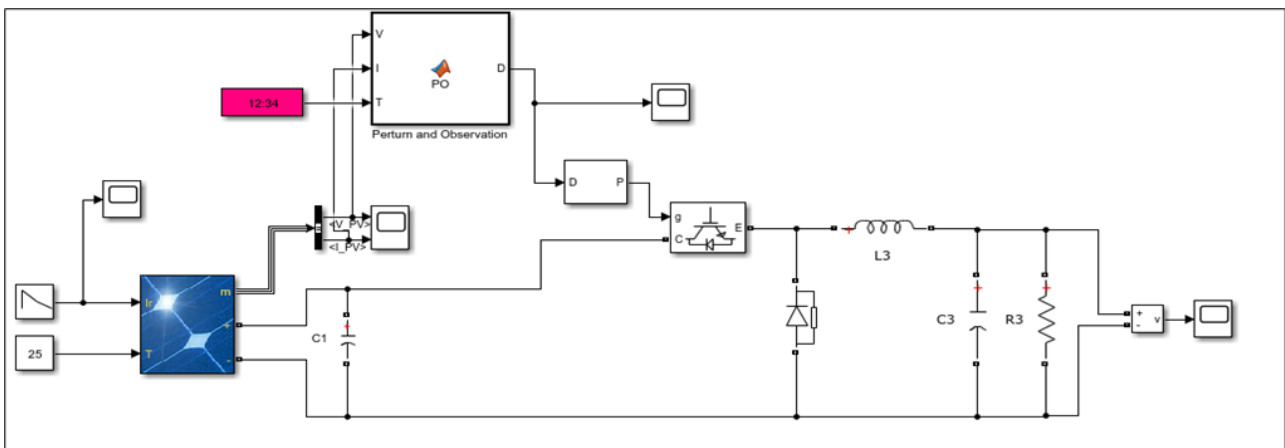


Figure 9 MPPT with PV Module

The output of Current and voltage for PV at MMP described in Figure 10.

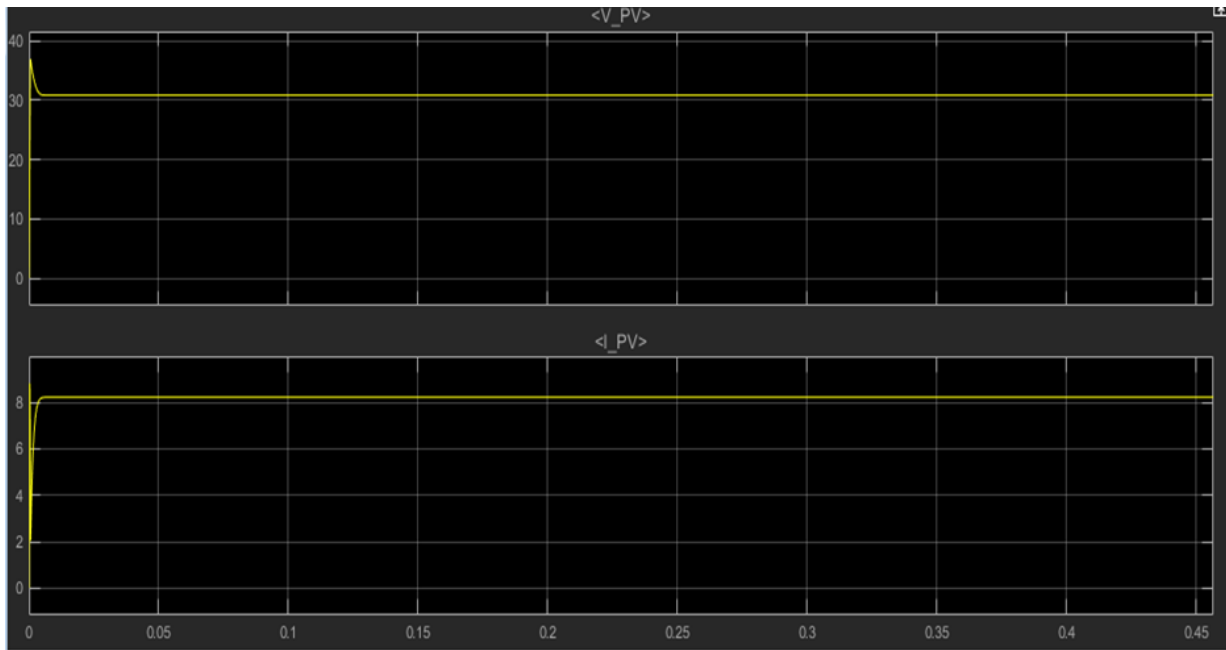


Figure 10 The output Current and voltage for PV

6.3. Inverter Controller

The Inverter controller is the most important component in this simulation because it can fulfil three synchronization conditions, to guarantee the active power flow from the PV, it consists of voltage loop which decide, where the active power will be injected to the utility grid and maintain the amplitude of output voltage equal to utility grid voltage, the second loop is current loop which insure that the current is flowing form the PV system to the grid. The frequency condition of synchronization will be fulfilled with PLL technic which can control the frequency of PWM of the inverter [18]. Before applying Park’s transformations, we should use the PU system so all the parameters will be the same type and can be controlled and adjusted. The nominal value of PV power is the base and utility grid voltage is the base for PU system. Figure 11 shows voltage loop in the controller.

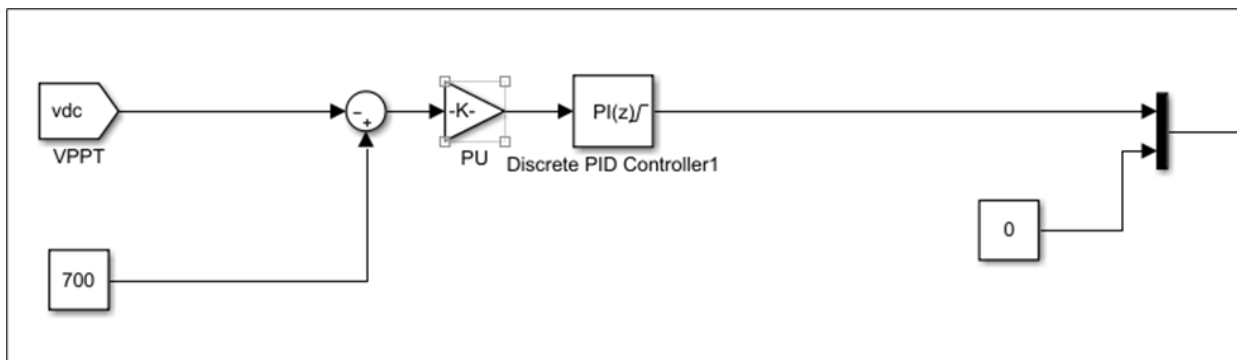


Figure 11 Voltage loop

The Figure 11 shows the output of PI controller is I_{d-ref} (the active power produced from PV system) and $I_{q-ref}=0$ because there isn't reactive power in the DC voltage and all the adjustment will be applied in active power through the current loop in the next step. Figure 12 shows Park’s transformations [19], PU calculations and current loop which compare the output Current of inverter with I_{d-ref} and I_{q-ref} then using PI controller to decide the adjustment needed in the output voltage in (d,q,0).

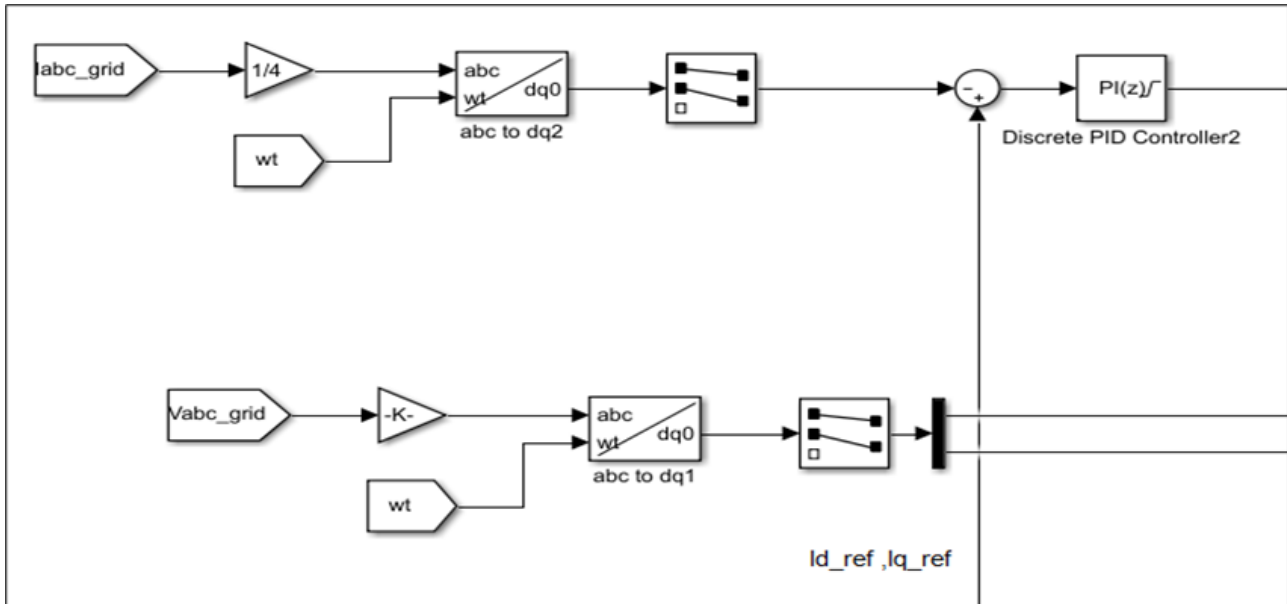


Figure 12 Park's transformations, PU calculations and current loop

The selector is used to eliminate the third sequence in (d,q,0) cause there is no need for it in normal conditions. The output of PI controller goes to output voltage for the inverter as adjustment signal. The (d,q) inverter voltage has been modeled as result of the value of grid voltage in (d,q) with the voltage drop in the coupling inductors as shown in Figure 13.

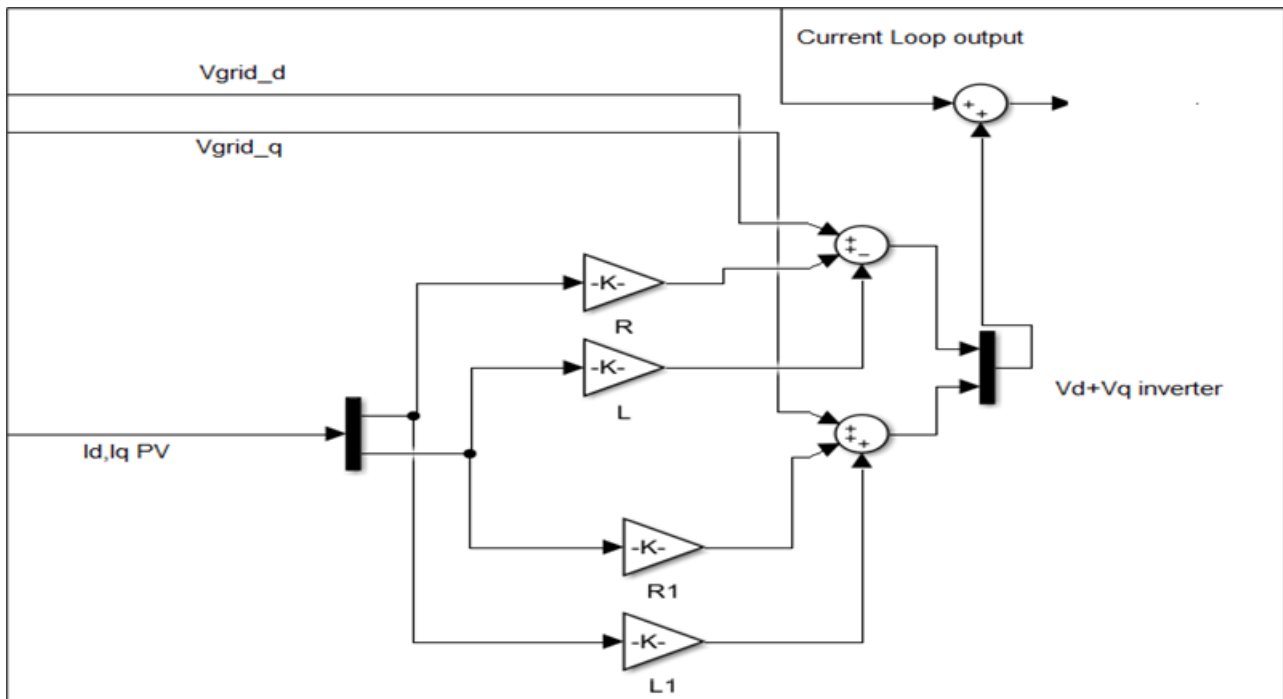


Figure 13 Modeling inverter output voltage in (d-q)

7. Case study

In the simulation we use a 66/20kV distribution power system with three phase and heap electrical loads, now we apply a 125kw PV system consist of 500 PV module with nominal power 250w, the PV array has 25 with Parallel strings , 20 Series-connected modules per string (25x20=500), these array works in MPPT with P&O algorithm through a Buck converters connected , with side of DC-link, the DC link is connected to the central inverter which will be the interface

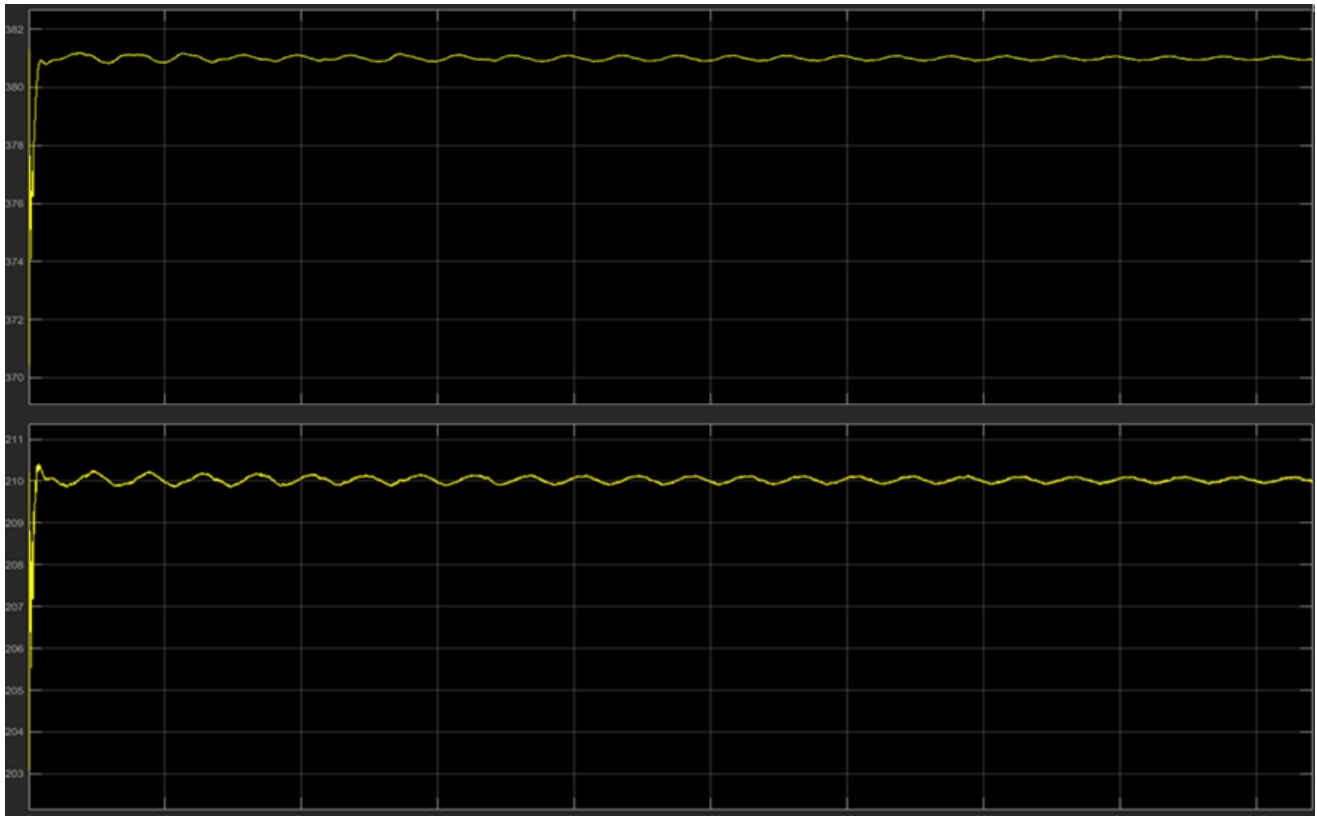


Figure 15 Active and reactive power produced from the grid

It's about 382 kW and 210kVAR flow through power lines in the grid. The frequency and voltage amplitude are the most important parameters and has to be in the acceptable range, in Figure 16 we can see that the three-phase ac voltage in the power lines and it's pure sine wave without THD and has a constant amplitude. In the second part in Figure 16 the frequency in the utility grid and it has value constant on 50Hz [20].

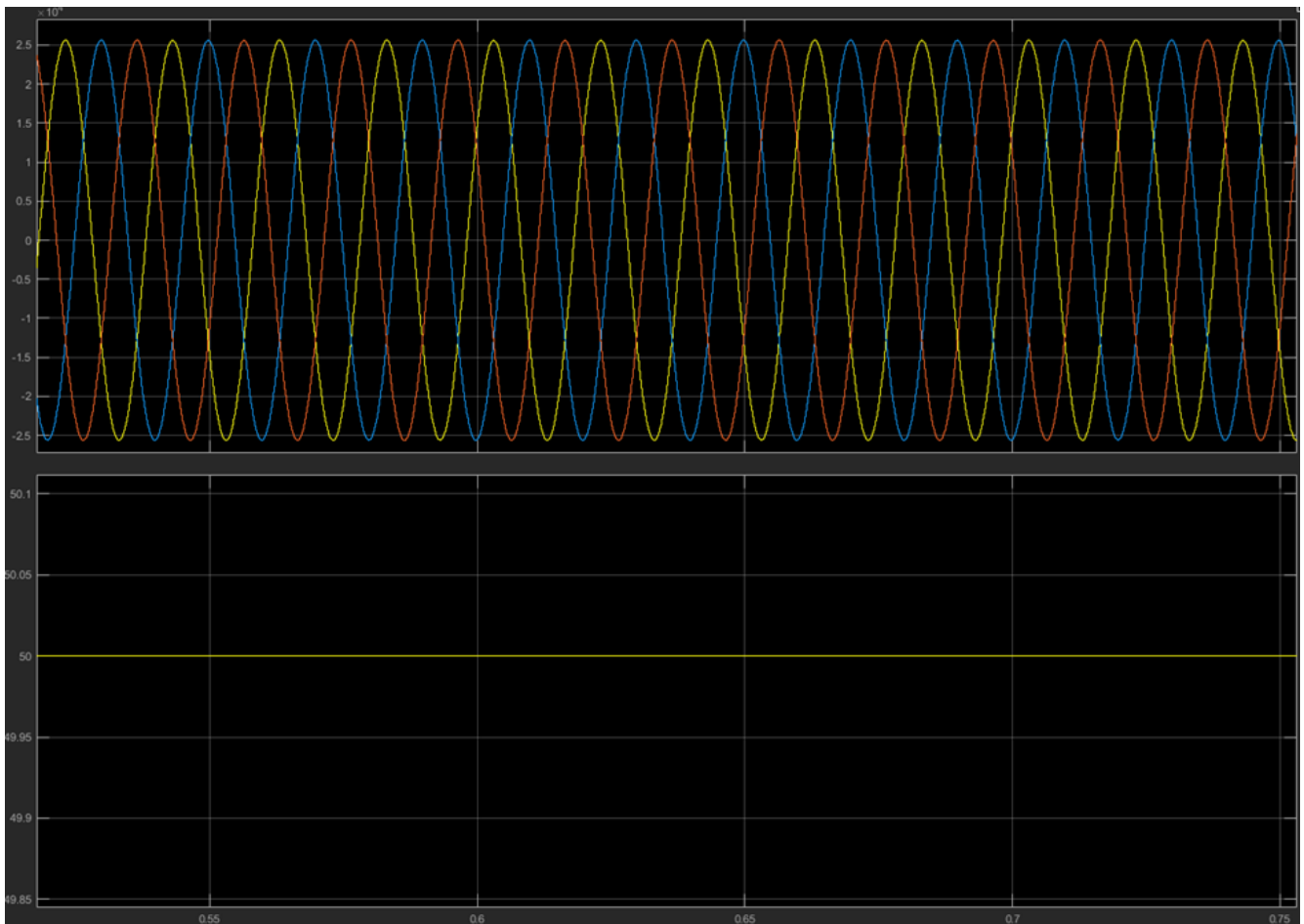


Figure 16 Voltage and frequency of utility grid

The overall current is shown in Figure 17, which will be used for judging the performance of PV system.

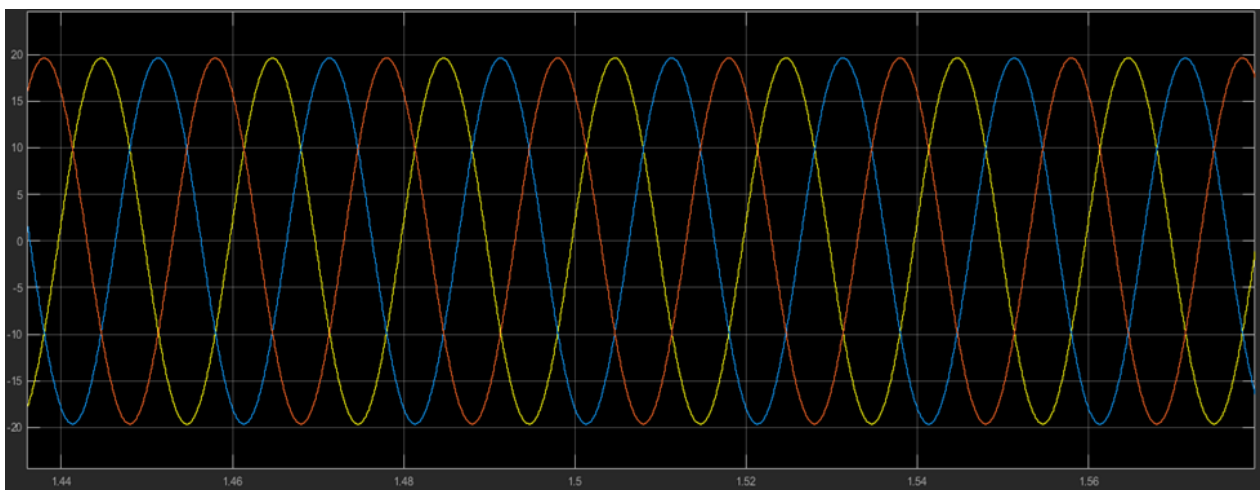


Figure 17 Overall current

7.2. After Synchronization

When we close the switchers the role of inverter will begin in fulfilling synchronization conditions, after a small transit state the PV system will produce active power, and it will flow in the utility grid. Figure 18 describes active power in kW and reactive power in kVAR flow in the grid after synchronization which will be less than the first state (Before synchronization) by the same amount of active power produced by the PV system.

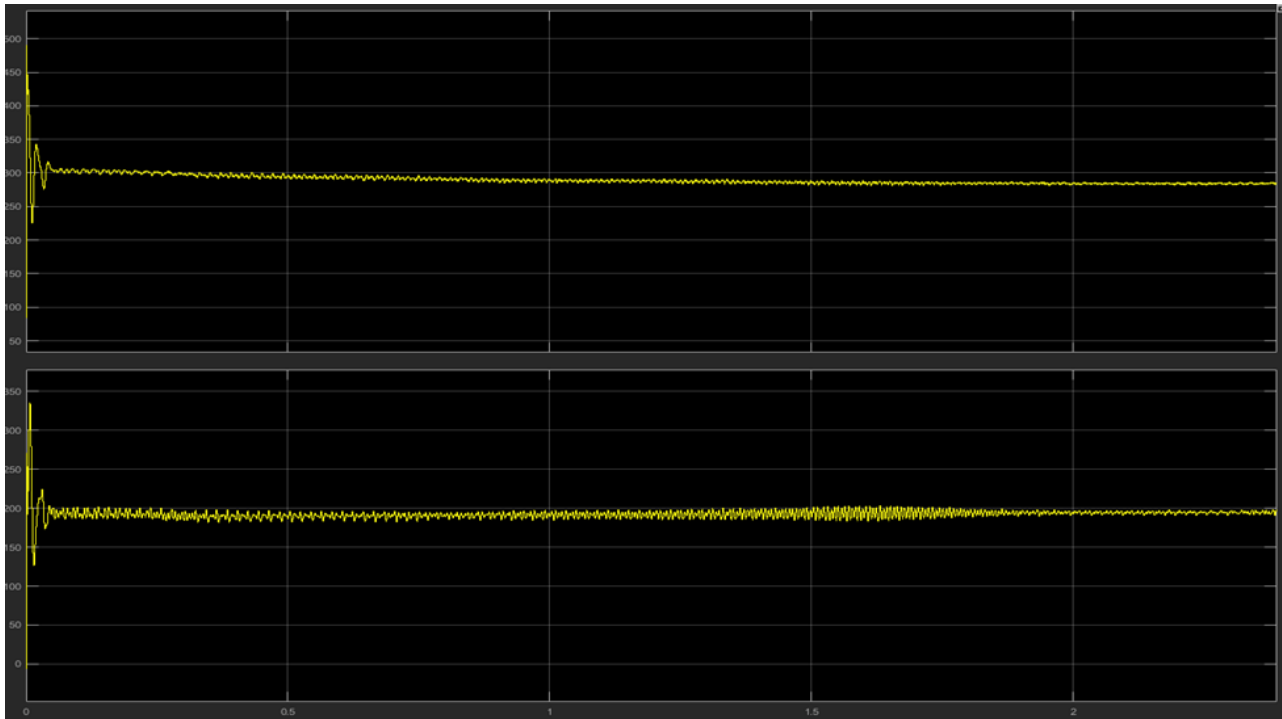


Figure 18 The active power in kW and reactive power

Synchronization the utility grid's active power was around 382kW and the reactive power was 210kVAR, now after the synchronization the active power from the utility We can see that the reactive power isn't affected a lot, because all the power injected by the PV system is active. The reactive power gets slightly less because the power losses in the power lines are getting lower due to the flow of active power from the PV reducing the active power flow in the Utility grid so. The active power produced from the utility grid decreased by the same amount of the power produced from the PV System, before the grid around 265kW and the reactive power 195kVAR, which indicates that using PV systems and disturbed generating can increase the capability of power lines to transport the active power, while decrease the power losses and reactive power flow in the grid.

Concerning the parameters of power system (Voltage - frequency) after synchronization, Figure 19 shows the voltage and frequency after injecting the power from PV system, and we can see that the voltage is 20kV RMS value and frequency is 50 Hz and stay in the acceptable range. In some Utility grid the renewable energy generating systems used to support the power system to maintain it's essential parameters in the nominal values through adjusting the power factor of the inverters of the renewable energy system which change the power flow in the grid to keep the voltage and frequency in the grid nodes in the nominal values.

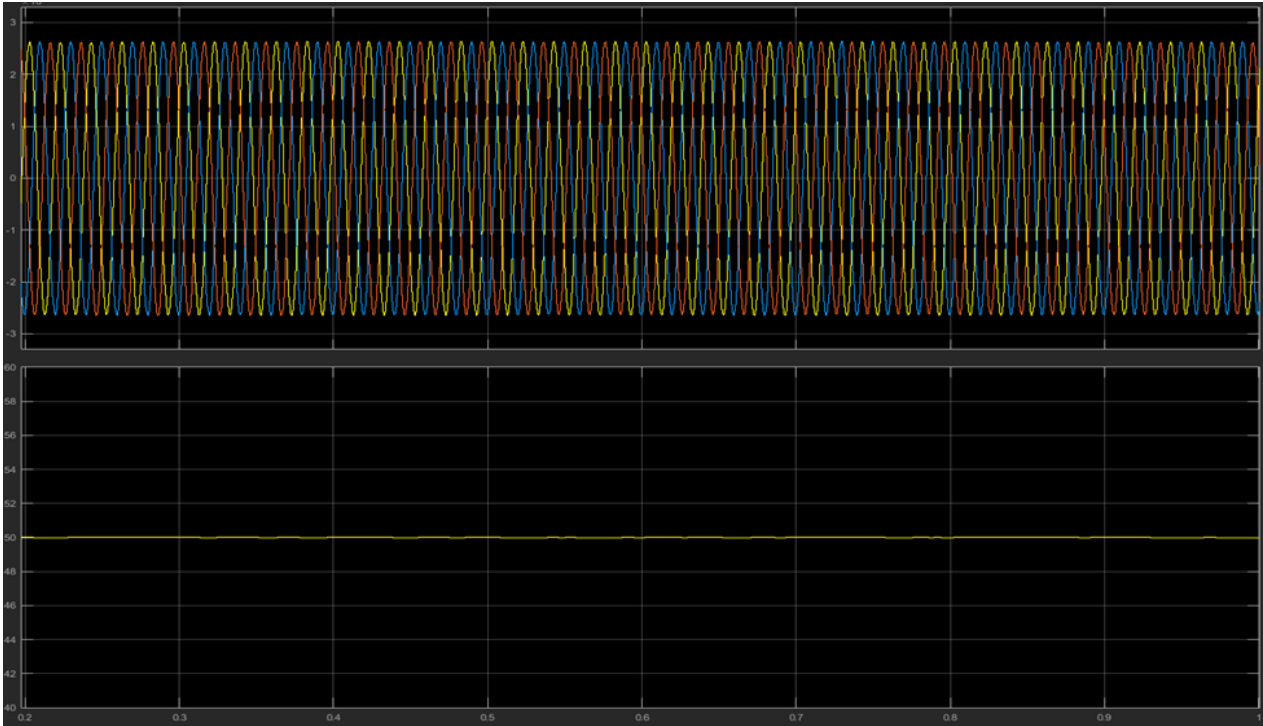


Figure 19 Voltage and frequency After synchronization

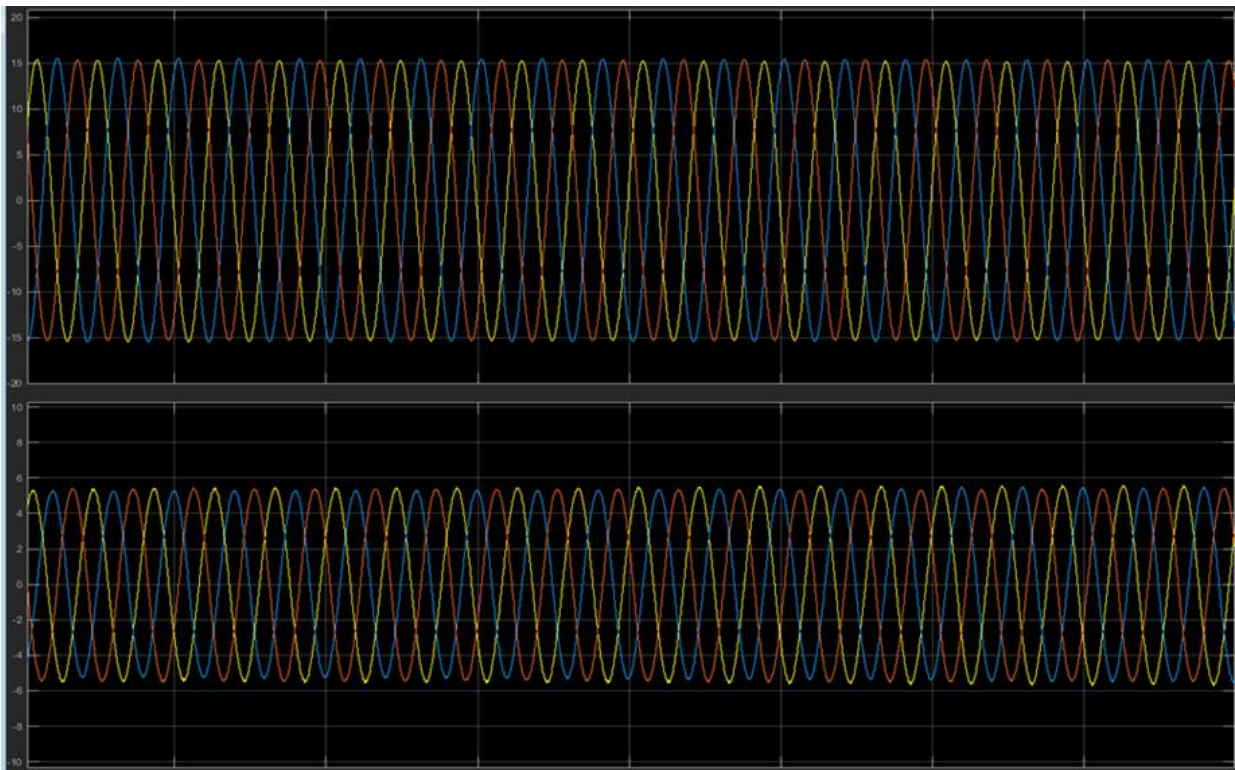


Figure 20 Current from the grid and current from PV after synchronization

As the power flow changes the current in the utility grid has to change in the same way, Figure 20 shows the current from the utility grid and the current production by PV cell, we can figure out that the utility grid decreased as the same amount of the current produced from the PV system. Before synchronization the current was about peak value 20 Amp on the 20kV side, after synchronization the current is peak value 15 Amp and the produced current from PV is peak value 5 Amp as shown in Figure 20.

8. Conclusion

Renewable energy-generating systems can participate in disturbed utility grids and produce active or reactive power according to the need of the system by changing the power factor of the working inverter. before synchronization utility grid produced 382 kW, 210kVAR and 20A peak value current and the frequency was 50Hz, after synchronization the photovoltaic system inject nearly 125kW and 5 A peak current and the frequency maintain 50Hz, so the load and current flow will change. The utility grid produces 265 kW, 195kVAR and 5A peak value current which indicates that the active power generated from PV system was injected in utility grid.

Compliance with ethical standards

Disclosure of conflict of interest

No conflict of interest to be disclosed.

References

- [1] R. Khezri and A. Mahmoudi, Review on the state-of-the-art multi-objective optimisation of hybrid standalone/grid-connected energy systems, *IET Gener. Transm. Distrib.*, vol. 14, no. 20, pp. 4285–4300, Oct. 2020, doi: 10.1049/iet-gtd.2020.0453.
- [2] M. K. H. Rabaia, C. Semeraro, and A.-G. Olabi, Recent progress towards photovoltaics' circular economy, *J. Clean. Prod.*, vol. 373, p. 133864, Nov. 2022, doi: 10.1016/j.jclepro.2022.133864.
- [3] Y. F. Nassar, H. J. El-khozondar, G. Ghaboun, M. Khaleel, Z. Yusupov, and Abdussalam Ahmed; Abdulgader Alsharif, Solar and Wind Atlas for Libya, *Int. J. Electr. Eng. Sustain.*, vol. 1, no. 3, pp. 27–43, 2023, [Online]. Available: <https://ijees.org/index.php/ijees/index>
- [4] A. A. Ahmed, A. Alsharif, T. Triwiyanto, M. Khaleel, C. W. Tan, and R. Ayop, Using of Neural Network-Based Controller to Obtain the Effect of Hub Motors Weight on Electric Vehicle Ride Comfort, 2022 IEEE 2nd Int. Maghreb Meet. Conf. Sci. Tech. Autom. Control Comput. Eng. MI-STA 2022 - Proceeding, pp. 189–192, 2022, doi: 10.1109/MI-STA54861.2022.9837608.
- [5] S. Rajasekaran, S. Suresh, A. Ramkumar, and K. Karthikeyan, A Novel Solar Photovoltaic Integrated Modified SEPIC High Gain DC–DC Converter Using Evolutionary Algorithms for Electric Vehicle Battery Applications, *J. Electr. Eng. Technol.*, vol. 18, no. 5, pp. 3681–3694, Sep. 2023, doi: 10.1007/s42835-023-01459-2.
- [6] J. S. Koh, R. H. G. Tan, W. H. Lim, and N. M. L. Tan, A Modified Particle Swarm Optimization for Efficient Maximum Power Point Tracking Under Partial Shading Condition, *IEEE Trans. Sustain. Energy*, vol. 14, no. 3, pp. 1822–1834, Jul. 2023, doi: 10.1109/TSTE.2023.3250710.
- [7] R. Dogga and M. K. Pathak, Recent trends in solar PV inverter topologies, *Sol. Energy*, vol. 183, no. February, pp. 57–73, May 2019, doi: 10.1016/j.solener.2019.02.065.
- [8] T. Sutikno, H. S. Purnama, N. S. Widodo, S. Padmanaban, and M. R. Sahid, A review on non-isolated low-power DC–DC converter topologies with high output gain for solar photovoltaic system applications, *Clean Energy*, vol. 6, no. 4, pp. 557–572, Aug. 2022, doi: 10.1093/ce/zkac037.
- [9] M. Salem, A. Jusoh, N. R. N. Idris, H. S. Das, and I. Alhamrouni, Resonant power converters with respect to passive storage (LC) elements and control techniques – An overview, *Renew. Sustain. Energy Rev.*, vol. 91, no. June, pp. 504–520, Aug. 2018, doi: 10.1016/j.rser.2018.04.020.
- [10] A. Sharma, H. P. Singh, and S. K. Sinha, Performance Enhancement of Integrated Solar-Wind Hybrid Energy System using MPPT, in 2018 3rd International Innovative Applications of Computational Intelligence on Power, Energy and Controls with their Impact on Humanity (CIPECH), IEEE, Nov. 2018, pp. 1–4. doi: 10.1109/CIPECH.2018.8724265.
- [11] A. H. Almalih, M. A. Faraj, and A. Nouh, Comparison between Global MPPT Techniques for PV Array Systems Subjected to Different Partially Shaded Conditions, in 2022 IEEE 2nd International Maghreb Meeting of the Conference on Sciences and Techniques of Automatic Control and Computer Engineering, MI-STA 2022 - Proceeding, 2022, pp. 673–679. doi: 10.1109/MI-STA54861.2022.9837668.

- [12] A. Chellakhi, S. El Beid, and Y. Abouelmahjoub, An improved adaptable step-size P&O MPPT approach for standalone photovoltaic systems with battery station, *Simul. Model. Pract. Theory*, vol. 121, p. 102655, Dec. 2022, doi: 10.1016/j.simpat.2022.102655.
- [13] A. Ballaji, N. Hediya, R. P. Mandi, and K. Narayana Swamy, Design and Implementation of Perturb and Observation Maximum Power point Transfer (MPPT) algorithm for Photovoltaic system, *J. Eng. Res. Appl. www.ijera.com*, vol. 8, no. May, pp. 16–23, 2018, doi: 10.9790/9622-0805021623.
- [14] N. Priyadarshi et al., Performance Evaluation of Solar-PV-Based Non-Isolated Switched-Inductor and Switched-Capacitor High-Step-Up Cuk Converter, *Electronics*, vol. 11, no. 9, p. 1381, Apr. 2022, doi: 10.3390/electronics11091381.
- [15] H. Oufettoul, S. Motahhir, G. Aniba, and I. Ait Abdelmoula, Comprehensive Analysis of MPPT Control Approaches under Partial Shading Condition, in *2022 11th International Conference on Renewable Energy Research and Application (ICRERA)*, IEEE, Sep. 2022, pp. 352–359. doi: 10.1109/ICRERA55966.2022.9935687.
- [16] A. Nadeem and A. Hussain, A comprehensive review of global maximum power point tracking algorithms for photovoltaic systems, *Energy Syst.*, vol. 14, no. 2, pp. 293–334, May 2023, doi: 10.1007/s12667-021-00476-2.
- [17] S. Ahmed, S. Mekhilef, M. B. Mubin, and K. S. Tey, Performances of the adaptive conventional maximum power point tracking algorithms for solar photovoltaic system, *Sustain. Energy Technol. Assessments*, vol. 53, p. 102390, Oct. 2022, doi: 10.1016/j.seta.2022.102390.
- [18] A. A. Al-Manfi, W. A. Mohamed, and E. F. Elsalhin, Voltage Control of Stand-alone Single Phase Self Excited Induction Generator for Variable Speed Wind Turbine Using Bang Bang-PWM Controller, in *2022 IEEE 2nd International Maghreb Meeting of the Conference on Sciences and Techniques of Automatic Control and Computer Engineering (MI-STA)*, IEEE, May 2022, pp. 749–754. doi: 10.1109/MI-STA54861.2022.9837503.
- [19] A. Sadick, Maximum Power Point Tracking Simulation for Photovoltaic Systems Using Perturb and Observe Algorithm, in *Solar Radiation - Enabling Technologies, Recent Innovations, and Advancements for Energy Transition [Working Title]*, IntechOpen, 2023. doi: 10.5772/intechopen.111632.
- [20] S. M. Masum, S. N. Rahman, M. M. Haque, and M. S. Rana, Performance analysis and simulation design of a soft switching Cuk DC/DC converter with controllers, in *2022 IEEE 2nd International Maghreb Meeting of the Conference on Sciences and Techniques of Automatic Control and Computer Engineering, MI-STA 2022 - Proceeding*, 2022, pp. 590–595. doi: 10.1109/MI-STA54861.2022.9837686.